# ChemComm

Accepted Manuscript


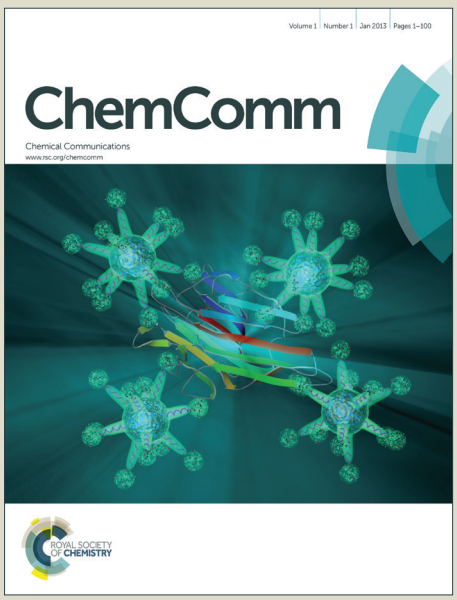





ROYAL SOCIETY OF CHEMISTRY

www.rsc.org/chemcomm

ChemComm RSCPublishing

COMMUNICATION

# Graphene Mediated Self-Assembly of Fullerene Nanorods

Tony J. Gnanaprakasa,[a] Deepak Sridhar,[b] Warren J. Beck,[c] Keith Runge,[a] Barrett G. Potter Jr.,[a] Thomas J. Zega[a,d] Pierre A. Deymier,[a] Srini Raghavan, [a,b] and Krishna Muralidharan[a,†]

**A simple procedure for solution-based self-assembly of $C_{60}$ fullerene nanorods on graphene substrates is presented. Using a combination of electron microscopy, X-ray diffraction and Raman spectroscopy, it is shown that the size, shape and morphology of the nanorods can be suitably modified by controlling the kinetics of self-assembly.**

$C_{60}$ fullerene based structural assemblies such as nanorods[1-5] (FNR), nanotubes[6-9] (FNT), nanowhiskers[9-16] (FNW), wires[17], disks[18,19], nanosheets[20] (FNS) and microribbons[5] (FMR) have been subjects of many recent investigations. In particular, FNR and FNT, which form when fullerenes ($C_{60}$) assemble along a growth axis parallel to a close-packed direction, exhibit remarkable physical and chemical properties potentially enabling a myriad of technological applications[1,5,9,15,21,22] including opto-electronic devices, catalysis, electrochemical devices and sensors. So far, liquid-liquid interface precipitation (LLIP) based methods have been the primary techniques of choice for fabrication of such structures[1-3, 11, 20]. In LLIP, a mixture of two solvents, one in which $C_{60}$ molecules are soluble, is used for forming fullerene nanostructures. In addition to LLIP, which is often a time-consuming process, slow evaporation of solvents containing dissolved fullerenes on substrates[10,23,24], as well as more complex and expensive methods have been developed for fabricating fullerene based assemblies; these include encapsulation within amphiphilic hexagonal porphyrin matrix,[21] controlled alignment of nanorods via cross-linking[22] and templated 'drip-and-dry' techniques.[25] As an alternative to these methods, we present a simple, straightforward and rapid process that relies on self-assembly for synthesizing faceted FNR, mediated by graphene-based substrates. Further, we demonstrate that the shape, size and morphology of the self-assembled fullerene structures can be suitably modified by controlling the kinetics of the self-assembly.

[a] *Department of Materials Science and Engineering,* [b] *Department of Chemical and Environmental Engineering,* [c] *Department of Physics,* [d] *Department of Planetary Sciences; The University of Arizona, Tucson, AZ – 85721, United States. Email: krishna@email.arizona.edu*

† Electronic Supplementary Information (ESI) available:

A key benefit that our method offers is the ability to couple and harness the unique properties of FNR's with that of graphene, opening new avenues for realizing hybrid carbon nanostructures with distinct structure-property relations.

The various stages involved in the self-assembly of fullerene structures are illustrated in Figure 1. The chemical components include (i) toluene solutions containing dissolved $C_{60}$ molecules and (ii) graphene grown via chemical vapor deposition (CVD) on 1 cm x 1 cm copper substrates. The synthesis procedure, which is carried out at room temperature, consists of dip-coating the graphene substrate in the toluene solution for fifteen minutes followed either by a static drying step or subjecting the dip-coated substrate to drying via a gentle pressurized air-stream (2 psig) for ten seconds. Specific information on the CVD process as well as the preparation of the toluene solution and the drying procedures is discussed in the supplementary information section.

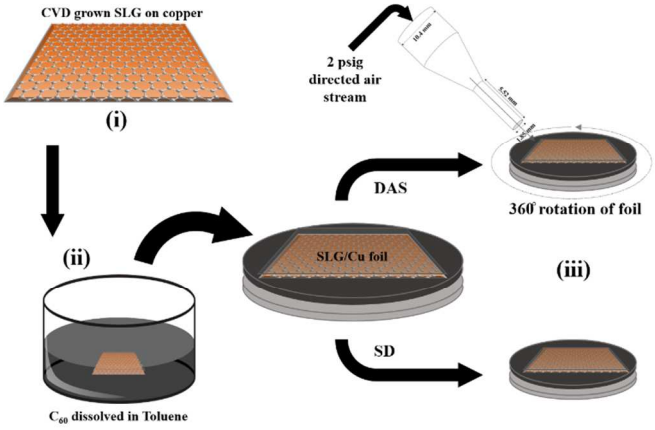


Figure 1: An illustration of the steps involved in the fullerene self-assembly procedure. Step (i) refers to CVD synthesis of single layer graphene (SLG) on copper; step (ii) involves dip-coating the SLG/copper substrate in a 2mg/ml fullerene dissolved in toluene solution; in step (iii), the dip-coated substrate is either statically dried or dried under a 2 psig directed air-stream using a 1.5 mm nozzle.

In addition, details on the different characterization techniques used for examining the self-assemblies obtained using the two drying procedures such as scanning electron microscopy, Raman

spectroscopy, and x-ray diffraction are also available in the supplementary information section.

The SEM images of fullerene assemblies obtained under the two different drying conditions are given in Figure 2(a-d) and Figure 3(a-d). For both procedures, namely static-drying (SD) and drying under a directed air-stream (DAS), self-assembly occurs in a rapid fashion, leading to the formation of DAS and SD structures within a minute and five minutes respectively. When dried under the DAS, uniformly sized, prismatic FNR are formed (Figure 2a-d). In contrast, SD yields a distribution of fullerene assemblies of differing geometries and sizes (Figure 3a-d). The DAS-FNR's are typically between 1--3 μm in length, 0.3-0.5 μm in diameter, and the major growth axis is parallel to the underlying substrate. An analysis of the size-distribution of the DAS-FNRs is provided in the supplementary information section (Fig. S2). In contrast, SD-self assemblies consist of needles, tubular and faceted rods and interconnected structures as shown in Figures 3(a-d). Their sizes and diameters range up to 100 μm and 5 μm respectively; some of the SD rods as shown in Figures 3(b-d), are incompletely formed and characterized by cracks, and some of the SD-rods are hollow (Figure 3b).

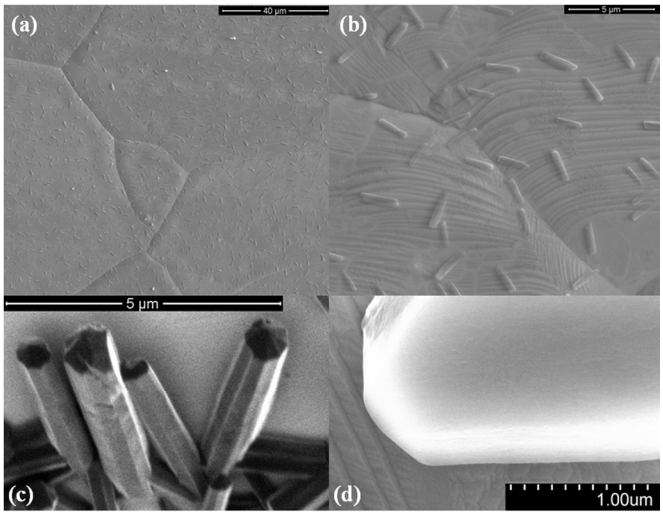


Figure 2: SEM micrographs of DAS-FNRs at different magnifications. The scale bars in (a), (b), (c) and (d) are 40 μm, 5 μm, 5 μm and 1 μm respectively. In (b) and (d) graphene wrinkles are clearly visible. The facets of the FNRs are visible in (c) and (d).

Also seen is a corrugated pattern found in the underlying graphene (Figures 2b and 2d as well as in Figures 3c and 3d). These corrugations consist of wrinkles (i.e. humps and valleys) that arise due to differences in thermal expansion coefficients and lattice parameters of the metal-substrate and graphene[26].

To characterize the structure of the self-assembled structures, Raman spectroscopy and x-ray diffraction (XRD) were carried out. The respective XRD patterns of the SD- and DAS-self assemblies are shown in Figure 4. SD-self assemblies reveal a face center cubic (FCC) crystalline structure with lattice parameter = 1.41 nm, which is typical of fullerene crystals. The XRD from the DAS-self assemblies, on the other hand, suggest a hexagonal close packing (hcp) crystalline structure with lattice parameters (i.e.. *a,c*) equalling 2.01 and 0.95 nm respectively. The differences in the respective crystalline structures can be attributed to the presence of solvent toluene molecules within the DAS-FNRs, which is known to stabilize the hexagonal structure during the self-assembly[11].

The Raman spectra of the respective structures are given in Figure 5. Distinct differences between the SD and DAS structures are seen in the high frequency peak positions and line-widths of the characteristic fullerene peaks associated with the Raman active vibrational modes $A_g2$, $H_g7$, and $H_g8$. Specifically, for the DAS spectra, multiple Lorentzian line shapes were required to ensure an accurate fit of these high frequency peaks, while the $A_g2$ peak was downshifted in addition to the appearance of satellite peaks in its vicinity. The narrower line-widths (given in Table 1) in the DAS spectra are indicative of a greater degree of organization in the self-assembled structures as compared to the SD structures. The split-peak characteristics of the high-frequency Raman modes for the DAS-FNRs are very similar to that of pressure-polymerized fullerene (PPF) and polymerized metallic alkali-$C_{60}$ orthorhombic structures[27], indicating the polymerization of the DAS-FNRs. While the peak position of the $A_g2$ peak is sensitive to photo-polymerization effects[16], the presence of the additional high-frequency split-peaks points to the fact that the DAS-FNRs were polymerized even prior to Raman studies.

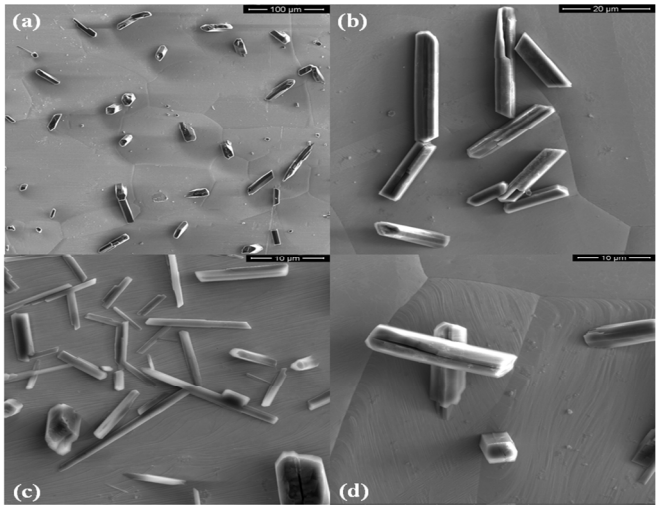


Figure 3: SEM micrographs of SD self-assemblies at different magnifications. The scale bars in (a), (b), (c) and (d) are 100 μm, 20 μm, 10 μm and 10 μm respectively. In (c) and (d) graphene wrinkles are clearly visible. Notice the variations in size, morphology and orientation of the ED self-assemblies.

An additional peak at 1622 $cm^{-1}$ in the DAS Raman spectrum, can be attributed to a characteristic C-C vibrational mode of toluene molecules. Based on Kapitán *et al*.,[28] the upshift of 17 $cm^{-1}$ in this peak can be regarded as a consequence of the reduction in symmetry of the underlying benzene ring, which arises due to chemical interactions between the FNRs and the confined toluene molecules.

In contrast, the SD-derived structures, display broad $H_g7$, $A_g2$ and $H_g8$ peaks, but do not show peak-splitting, indicating the lack of polymerization during the self-assembly or during the Raman studies. Further, as discussed by Satish et al.,[3], the shift in the $A_g2$ peak-position (by 12 $cm^{-1}$ using pristine monomeric $C_{60}$ as reference) is attributed to strain within the SD-structure. This is inferred based on the fact that the SD-self assemblies crystallize in



 

an FCC structure. Thus, it can be assumed that the SD-structures are not polymerized, while significant strain is present within these structures, which leads to the shift in $A_g2$ peak position. Another striking difference between SD- and DAS-structures is the presence of a broad peak at 1357 $cm^{-1}$ in the SD spectrum. This peak is characteristic of amorphous carbon, which is known to be formed when open fullerene assemblies are photon-irradiated (from the Raman laser) in the presence of oxygen[12]. Since some of the SD-self assemblies are incompletely formed as seen in Figure 3, it can be inferred that these structures contain oxygen, leading to the formation of amorphous carbon during the Raman studies. The comparison in peak positions and the line-widths (i.e. full width half max (FWHM)) for the DAS-FNRs structures with SD-structures is given in Table 1.

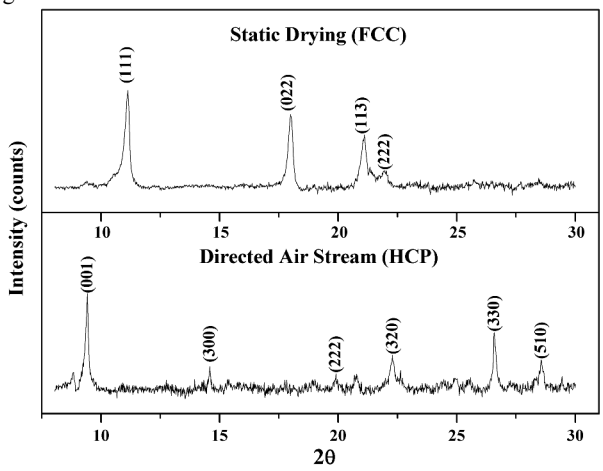


Figure 4: Indexed XRD patterns of the SD and DAS crystal structures. The SD and DAS structures are indexed by FCC and HCP systems respectively.

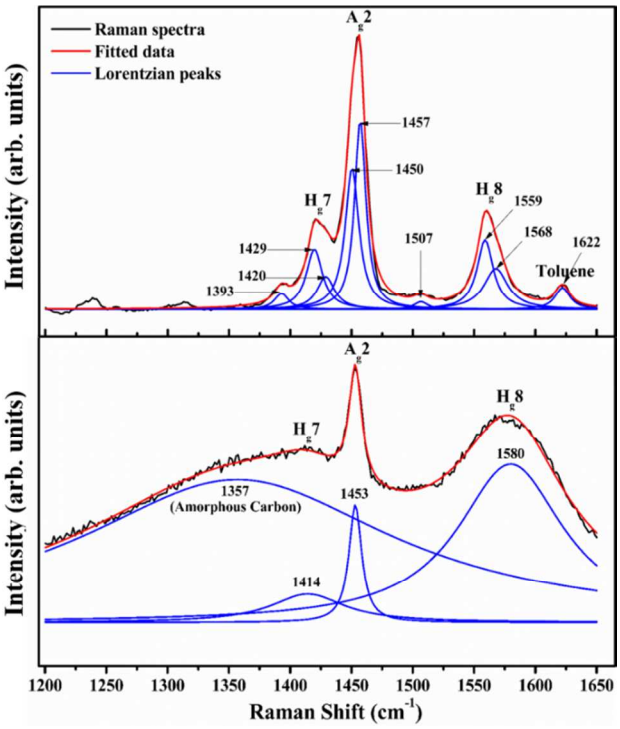


Figure 5: Raman spectra of (a) DAS-derived and (b) SD-derived structures. Notice the differences in the number of Lorentzians required to ensure an accurate fit for both cases.

Table 1: Raman peak positions, peak widths and peak heights of DAS and SD structures.

| $cm^{-1}$ | DAS peaks | | | SD peaks | | |
|---|---|---|---|---|---|---|
| | Position | Width | Height | Position | Width | Height |
| $H_g7$ | 1393 | 14 | 267 | 1414 | 73 | 140 |
| | 1420 | 16 | 1003 | | | |
| | 1429 | 17 | 548 | | | |
| $A_g2$ | 1450 | 14 | 2339 | 1453 | 13 | 582 |
| | 1457 | 11 | 3147 | | | |
| | 1507 | 14 | 129 | | | |
| $H_g8$ | 1559 | 16 | 1155 | 1580 | 106 | 782 |
| | 1568 | 24 | 680 | | | |
| Amorphous Carbon | | | | 1357 | 313 | 706 |
| Toluene | 1622 | 15 | 361 | | | |

The differences in size, structure and morphology of DAS and SD derived structures as discerned from the SEM, XRD and Raman analysis, clearly point to the importance of the drying method. In addition, recent investigations using scanning tunnelling microscopy have shown that the valleys within the corrugations, characteristic of graphene when grown on metal-substrates, enable strong adsorption of evaporatively deposited monolayers of $C_{60}$ molecules[29], leading to the formation of nanometric, aligned $C_{60}$ aggregates. Further, Sygula *et al*.,[30] have pointed out that toluene promotes self-assembly of $C_{60}$ molecules on carbon structures with curvature, and incorporates itself within the self-assembled nano-columns/chains. Based on these observations, the nucleation and growth of the self-assemblies can be explained as follows: the underlying graphene corrugations serve as nucleation sites for self-assembly of $C_{60}$ molecules into initial aggregates (nuclei). During growth of the nuclei, in the case of SD, the slower evaporation rate of toluene enables the majority of the aggregates to grow into larger self-assemblies as a result of short-range diffusion of $C_{60}$ molecules within the evaporating toluene film. This mechanism also leads to some of these self-assemblies serving as nucleation sites for the growth of secondary structures. Further, the fact that some of the larger self-assemblies are incompletely formed suggests that the growth was limited by the lack of long-range diffusion of $C_{60}$ molecules. This conclusion is further strengthened by the presence of much smaller tubes, needles and platelets, for which the growth must be similarly diffusion constrained. On the other hand, the relative abundance of similar DAS-FNRs that are smaller in size as compared to typical SD-structures indicates that the air-stream impacts the kinetics of self-assembly and induces the relatively rapid evaporation of toluene. In particular, the impinging air-stream disperses the continuous toluene film into smaller droplets, within which the dissolved $C_{60}$ molecules self-assemble to form distinct FNR structures as the solvent evaporates. A visual inspection demonstrated that the toluene droplets completely evaporated within a minute of DAS-drying as compared to a few minutes under SD conditions. Further, the rapid time-scales associated with the DAS-drying and self-assembly leads to the trapping of solvent molecules within the DAS-FNRs as confirmed by the XRD and Raman data. Interestingly, the DAS-FNRs are similar to the prismatic structures identified in Wei *et al*.,[5] which were obtained using LLIP. In Wei *et al*.,[5] it was shown that prismatic rods represent energy minimum fullerene self-assemblies. However, the LLIP procedure resulted in much longer times for the

formation of rods (~ two weeks), in contrast to the rapid, near-instantaneous FNR synthesis attained in this work.

A comparison with similar studies that have examined fullerene self-assembly on substrates reveals important distinctions as well as some similarities with respect to the respective self-assemblies. While Yao *et al*.,[23] observed different structures such as rods, platelets and micro-crystals on silicon, silica and aluminium, typically the self-assemblies occurs over hours, possibly due to the higher boiling point of the halogen-containing aromatic solvents (as compared to toluene). Heating the solvent as a means of hastening evaporation was examined, which resulted in a plethora of size and shapes of the self-assemblies. Wang et al.[10] have shown the ability to synthesize nanorods that vary between 80-500 nm in diameter using xylene as the solvent on many substrates (silica, silicon, molybdenum), but the nanorods were either cylindrical or had a rectangular cross-section unlike the prismatic FNRs derived in this work. Further, the time-scale of self-assembly corresponded to a few hours. Sallgren *et al*.,[24] were able to obtain a distribution of microcrystals and cylindrical needles and rods, by evaporating $C_{60}$ in benzene solutions on copper, while Tiwari *et al*.,[4], using toluene, synthesized rod-like crystals on molybdenum. In the latter two cases, information on the time-scale of the self-assembly process is not available. Finally, to compare and contrast the role of the substrate on fullerene self-assembly under similar SD and DAS conditions, experiments were carried out using copper foils as the substrate. Under DAS conditions, the predominant structure consisted of irregularly shaped sub-micron sized self-assemblies while under SD conditions, the shape and size of the self-assemblies ranged from sub-micron to 10's of microns. SEM images of self-assemblies derived on copper foils are given in the supplementary information section (Fig. S3).

A primary distinction between the above described studies and self-assembly on graphene is the fact that prismatic, equi-sized FNRs can be controllably obtained on graphene in much less time. This can be attributed to the choice of CVD grown graphene on copper as the substrate along with the choice of toluene as the solvent, both of which combine to promote the formation of stable aggregates that serve as nuclei, enabling the growth of FNRs, when subjected to the directed air-stream. Further the DAS-FNRs are characterized by their ability to be polymerized during self-assembly, , in contrast to the SD-structures as well as structures obtained in the studies of Yao *et al*.,[23], Wang *et al*.,[10], Sallgren *et al*.,[24] and Tiwari *et al*.,[4], which were not susceptible to polymerization.

In conclusion, we have demonstrated a facile synthesis procedure for fabricating faceted polymerized fullerene nanorods on graphene based substrates. The ability to reliably control the spatial distribution, size, shape, morphology as well as the chemistry of the self-assembled fullerene nanorods in an inexpensive fashion using a directed air-stream, represents a rapid alternative to existing procedures. The adopted procedure allows for ready integration of fullerene self-assemblies with graphene, opening up new avenues for harnessing and exploiting the unique structure-property relations of these carbon nanostructures.

This work was supported by grants from the Renewable Energy Network at the University of Arizona and NSF-DMR (1148936). We thank Dr. Sue A. Roberts for the XRD results as well as Dr. Douglas A. Loy and Dr. Kaushik Balakrishnan for useful discussions.

## References

1. Y. Xu, J. Guo, T. Wei, X. Chen, Q. Yang and S. Yang, *Nanoscale*, 2013, **5**, 1993
2. L. C. Chong, J. Sloan, G. Wagner, S. R. P. Silva and R. J. Curry, *J. Mater. Chem.*, 2008, **18**, 3277
3. M. Sathish, K. Miyazawa, J. P. Hill and K. Ariga, *J. Am. Chem. Soc.*, 2009, **131**, 6372
4. R. N. Tiwari, M. Ishihara, J. N. Tiwari and M. Yoshimura, *Chem. Comm.*, 2012, **48**, 3003
5. L. Wei, J. Yao and H. Fu, *ACS Nano*, 2013, **7**, 7573
6. J. Minato, K. Miyazawa and T. Suga, *Sci. Technol. Adv. Mat.*, 2005, **6**, 272
7. Y. J. Xing, G. Y. Jing, J. Xu, D. P. Yu, H. B. Liu and Y. L. Li, *Appl. Phys. Lett.*, 2005, **87**, 263117
8. D. Liu, M. Yao, Q. Li, W. Cui, B. Zou, T. Cui, B. Liu, B. Sundqvist, T. Wagberg, *CrystEngComm*, 2011, **13**, 3600
9. K. Miyazawa, *Inorganic and Metallic Nanotubular Materials*, ed. T. Kijima, Springer, Berlin Heidelberg, 2010, vol. 117, ch. 15, pp. 201
10. L. Wang, B. Liu, D. Liu, M. Yao, Y. Hou, S. Yu, T. Cui, D. Li, G. Zou, A. Iwasiewicz and B. Sundqvist, *Adv. Mater.*, 2006, **18**, 1883
11. L. K. Shrestha, J. P. Hill, T. Tsuruoka, K. Miyazawa and K. Ariga, *Langmuir*, 2013, **29**, 7195
12. G. Li, Z. Han, G. Piao, J. Zhao, S. Li and G. Liu, *Mater. Sci. Eng. B*, 2009, **163**, 161
13. C. Li, B. Wang, Y. Yao, G. Piao, L. Gu, Y. Wang, X. Duan and R. Yu, *Nanoscale*, 2014, **6**, 6585
14. K. Ogawa, T. Kato, A. Ikegami, H. Tsuji, N. Aoki, Y. Ochiai and J. P. Bird, *Appl. Phys. Lett.*, 2006, **88**, 112109
15. K. Asaka, T. Nakayama, K. Miyazawa and Y. Saito, *Carbon*, 2012, **50**, 1209
16. M. Sathish and K. Miyazawa, *CrystEngComm*, 2010, **12**, 4146
17. J. Geng, W. Zhou, P. Skelton, W. Yue, I. A. Kinloch, A. H. Windle and B. F. G. Johnson, *J. Am. Chem. Soc.*, 2008, **130**, 2527
18. H. S. Shin, S. M. Yoon, Q. Tang, B. Chon, T. Joo and H. C. Choi, *Angew. Chem. Int. Ed.*, 2008, **47**, 693
19. Z. Tan, A. Masuhara, H. Kasai, H. Nakanishi and H. Oikawa, *Carbon*, 2013, **64**, 370
20. M. Sathish and K. Miyazawa, *J. Am. Chem. Soc.*, 2007, **129**, 13816
21. T. Hasobe, A. S. D. Sandanayaka, T. Wada and Y. Araki, *Chem. Comm.*, 2008, **29**, 3372
22. C-Y. Chang, C-E. Wu, S-Y. Chen, C. Cui, Y-J. Cheng, C-S. Hsu, Y-L. Wang and Y. Li, *Angew. Chem. Int. Ed.*, 2011, **50**, 9386
23. M. Yao, B. M. Anderson, P. Stenmark, B. Sundqvist, B. Liu and T. Wögberg, *Carbon*, 2009, **47**, 1181
24. J. Sallgren, H. Wang, S. L. Leonard, Y. H. Hu, *J. Phys. Chem. Solids*, 2012, **73**, 1070
25. H. Liu, Y. Li, L. Jiang, H. Luo, S. Xiao, H. Fang, H. Li, D. Zhu, D. Yu, J. Xu and B. Xiang, *J. Am. Chem. Soc.*, 2002, **124**, 13370
26. J. Wintterlin and M. L. Bocquet, *Surf. Sci.*, 2009, **603**, 1841
27. J. Winter, H. Kuzmany, A. Soldatov, P-A. Persson, P. Jacobsson, B. Sundqvist, *Phys. Rev. B.*, 1996, **54**, 17486
28. J. Kapitán, L. Hecht and P. Bouř, *Phys. Chem. Chem. Phys.*, 2008, **10**, 1003
29. J. Lu, P. S. E. Yeo, Y. Zheng, Z. Yang, Q. Bao, C. K. Gan and K. P. Loh, *ACS Nano*, 2012, **6**, 944
30. A. Sygula, F. R. Fronczek, R. Sygula, P. W. Rabideau and M. M. Olmstead, *J. Am. Chem. Soc.*, 2007, **129**, 3842



 